Multispectral Image Data Compression Using Classified Prediction and KLT in Wavelet Transform Domain

Tae-Su Kim, Seung-Jin Kim, Byung-Ju Kim, Jong-Won Lee,
Seong-Geun Kwon, and Kuhn-Il Lee
School of Electrical Engineering and Computer Science, Kyungpook National University
1370, Sankyug-Dong, Buk-Gu, Daegu 702-701, Republic of Korea
Tel: +82-53-950-5512, Fax: +82-53-950-5505
E-mail: myself21c@hotmail.com

Abstract: The current paper proposes a new multispectral image data compression algorithm that can efficiently reduce spatial and spectral redundancies by applying classified prediction, a Karhunen-Loeve transform (KLT), and the three-dimensional set partitioning in hierarchical trees (3-D SPIHT) algorithm in the wavelet transform (WT) domain. The classification is performed in the WT domain to exploit the interband classified dependency, while the resulting class information is used for the interband prediction. The residual image data on the prediction errors between the original image data and the predicted image data is decorrelated by a KLT. Finally, the 3D-SPIHT algorithm is used to encode the transformed coefficients listed in a descending order spatially and spectrally as a result of the WT and KLT. Simulation results showed that the reconstructed images after using the proposed algorithm exhibited a better quality and higher compression ratio than those using conventional algorithms.

1. Introduction

Some of the important applications of multispectral images include environmental assessment and monitoring, geology, agriculture, military surveillance, and natural resource management. A single multispectral image collected by the Landsat TM sensor has seven different bands and the volume of this data increases when multispectral images have a better spatial and spectral resolution. Therefore, efficient compression of such a large volume of multispectral image data is required for available communication channels and storage capacities. Multispectral images include both spatial and spectral redundancies. A number of techniques have already been proposed to reduce spatial and spectral redundancies and can be roughly classified into three types: (1) vector quantization (VQ), (2) prediction, and (3) transform coding, such as a WT, discrete cosine transform (DCT), and KLT. Recent papers on multispectral image data compression have applied these techniques.

Gupta *et al.*[1] proposed the use of VQ to reduce spatial redundancies using spatial blocks, and nonlinear block prediction to reduce spectral redundancies. Yet multispectral images are characterized by highly nonlinear dependencies. As such, this algorithm is not optimal due to incorrectness resulting from block prediction without classification.

Gelli *et al.*[2] carried out a pixel-by-pixel classification based on VQ to efficiently exploit the linear and nonlinear dependencies among the image bands. After the classification step, the spectral and spatial redundancies are exploited by performing a KLT in the spectral domain and DCT in the spatial domain. However, a lot of side class information has to be encoded after the pixel-by-pixel classification in the spatial domain.

Dragotti *et al.*[3] used a WT to reduce the spatial redundancies and KLT to reduce the spectral redundancies. The coefficients are first decorrelated spatially and spectrally and then encoded using the 3-D SPIHT algorithm.[4],[5] However, this algorithm does not consider classified interband dependency and the KLT is only used to reduce the interband redundancy in the WT domain.

Accordingly, a new multispectral image data compression algorithm is proposed that can efficiently reduce both spatial and spectral redundancies. A block diagram of the proposed algorithm is shown in Fig. 1. The feature band resulting from a WT is first encoded by the 2D-SPIHT algorithm. Then, all the other bands, except for the feature band, are predicted using a prediction. In other words, a WT is used to reduce the redundancies in the spatial domain, while classified prediction and a KLT are used to reduce the redundancies in the spectral domain. Finally, the transformed coefficients listed in a descending order spatially and spectrally are encoded by the 3D-SPIHT algorithm. Simulation results using Landsat TM image data confirmed the improved quality of the proposed algorithm as regards the average PSNR at an equal bit rate.

2. Proposed Algorithm

2.1 WT and Feature Band Selection

The multispectral image data X is represented as

$$X = \{X_1, X_2, X_3, \cdots, X_n\} \tag{1}$$

where the subscript n denotes the number of bands, n equals seven in the case of Landsat TM, X_1, X_2, and X_3 represent images in the visible spectral region, and X_4, X_5, X_6, and X_7 represent images in the infrared spectral region. Plus, X_6 is a thermal band with a different spatial resolution, which is considered separately. The multispectral image data W after a WT is represented as

$$W = \{W_1, W_2, W_3, \cdots, W_n\} \tag{2}$$

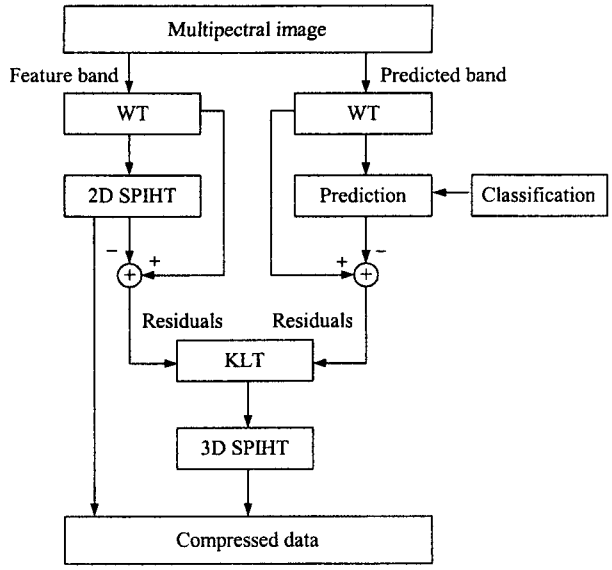

Fig. 1. Block diagram of proposed algorithm.

and the wavelet coefficient vector $W^b(i,j)$ with the same spectral location (i,j) of subband b is represented as

$$W^b(i,j)=[\, w_1^b(i,j), w_2^b(i,j),\cdots, w_n^b(i,j)\,] \tag{3}$$

where $0 \le b \le 12$ in the case of a four-level WT. Fig. 2 shows that the wavelet coefficient vector in the baseband can be represented as

$$W^0(i,j)=[\, w_1^0(i,j), w_2^0(i,j),\cdots, w_n^0(i,j)\,] \tag{4}$$

The selected feature band should have a low spatial variance and high correlation with the other bands. Therefore, after calculating the spatial variance and interband correlation in the baseband, band 2 was selected as the feature band. The selected feature band 2 was then encoded using the 2-D SPIHT algorithm in order to predict the other bands.

2.2 Classification in WT Domain

Multispectral image data in the WT domain has an energy

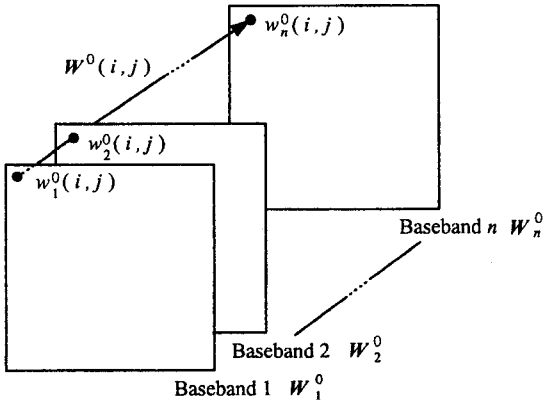

Fig. 2. Wavelet coefficient vector $W^0(i,j)$ in baseband.

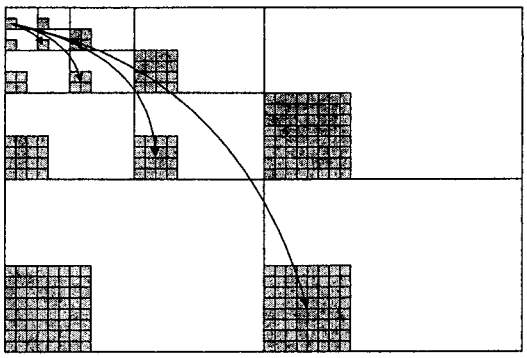

Fig. 3. Extension of class information in baseband to other subbands.

concentration in the baseband, and the wavelet coefficient vector $W^0(i,j)$ has different values according to the reflective characteristics of various regions. Thus, typical values can be obtained to classify regions using the generalized Lloyd method and these values then used as reference values for classification. The classification is arranged into classes that minimize the difference value between an input vector and the reference values. The class decision that assigns a wavelet coefficient vector into one of four regions is shown as

$$C = \arg\left[\min\left(\sum_{k=1}^{n} \left| W_k - Class_k^1 \right|^2, \sum_{k=1}^{n} \left| W_k - Class_k^2 \right|^2, \sum_{k=1}^{n} \left| W_k - Class_k^3 \right|^2, \sum_{k=1}^{n} \left| W_k - Class_k^4 \right|^2 \right) \right] \tag{5}$$

where $Class_k^1$ denotes a typical value for class 1 in the k-th band. The class information is then extended to other subbands by considering the spatial correlation and resolution, as shown in Fig. 3.

2.3 Classified Interband Prediction

The interband prediction using prediction coefficients is carried out for the other bands, except for feature band 2. Those wavelet coefficients that belong to the same class have the same interband linear dependency. In other words, the predicted value $\tilde{W}_p^b(c)$ can be represented by the prediction coefficients $A_p^b(c)$ and $B_p^b(c)$.

$$\tilde{W}_p^b(c) = A_p^b(c)\cdot \hat{W}_{ref}^b(c) + B_p^b(c) \tag{6}$$

$$A_p^b(c) = \frac{COV(W_{ref}^b(c), W_p^b(c))}{VAR(W_{ref}^b(c))} \tag{7}$$

$$B_p^b(c) = E[W_p^b(c)] - A_p^b(c)\cdot(E[W_{ref}^b(c)]) \tag{8}$$

where subscript p and ref indicate the predicted band and feature band, respectively, superscript b denotes the subband, c represents the class information, and

$E[\cdot]$, $COV(\cdot)$, and $VAR(\cdot)$ represent the expectation, covariance, and variance, respectively. The fixed prediction coefficients are calculated using various training images. When compared to the method that uses a self-image, the selection of fixed prediction coefficients in the proposed method has the advantage that no side information is needed.

2.4 Residual Image Data Encoding

The feature band image data encoded after the 2D SPIHT and predicted band image data both include errors when compared with the original image data. However, since this error image data still has an interband correlation, a spectral KLT[6],[7] is carried out to decorrelate the transformed coefficients, thereby reducing the spectral redundancies. The KLT is actually carried out subband-to-subband, rather than band-to-band. The number of the $n \times n$ covariance matrix is equivalent to that of the subbands in one band.

The wavelet coefficients vectors $\boldsymbol{W}$ with n bands can be expressed as

$$\boldsymbol{W} = [\, w_1, w_2, \cdots, w_n \,]^T \tag{9}$$

where w_i is the component of the i-th band of the wavelet coefficients vectors $\boldsymbol{W}$ and $[\cdot]^T$ denotes the transpose. The band-to-band covariance matrix is defined as

$$\boldsymbol{C}_W = \frac{1}{M} \sum_{k=0}^{M-1} \{[(\boldsymbol{W} - \boldsymbol{M}_W)(\boldsymbol{W} - \boldsymbol{M}_W)^T]\} \tag{10}$$

where M represents the number of the wavelet coefficients vecotors and the mean vector $\boldsymbol{M}_W$ is

$$\boldsymbol{M}_W = \frac{1}{M} \sum_{k=0}^{M-1} \boldsymbol{W} \tag{11}$$

The transformation matrix $\boldsymbol{T}$ is represented as

$$\boldsymbol{T} = [\boldsymbol{e}_1, \boldsymbol{e}_2, \cdots, \boldsymbol{e}_n]^T \tag{12}$$

where $\boldsymbol{e}_1 \sim \boldsymbol{e}_n$ are eigenvectors of $\boldsymbol{C}_W$ and the wavelet coefficients vectors $\boldsymbol{W}$ are trasformed by this transformation matrix $\boldsymbol{T}$. The transformed $\boldsymbol{Y}$ vectors are represented as

$$\boldsymbol{Y} = \boldsymbol{TW} = [\, y_1, y_2, \cdots, y_n \,]^T \tag{13}$$

where $y_1, y_2, \cdots, y_n$ are decorrelated, since the covariance matrix of $\boldsymbol{Y}$ is

$$\boldsymbol{C}_Y = \boldsymbol{T}\boldsymbol{C}_W\boldsymbol{T}^{-1} = \begin{bmatrix} \lambda_1 & 0 & \cdots & 0 \\ 0 & \lambda_2 & \cdots & 0 \\ \vdots & \vdots & \ddots & \vdots \\ 0 & 0 & \cdots & \lambda_n \end{bmatrix} \tag{14}$$

where $\lambda_1 \geq \lambda_2 \geq \cdots \geq \lambda_n$

As a result of the KLT, the coefficients are listed spectrally in a descending order of their eigenvalue magnitude. As a result of the WT and KLT, the significant coefficients are usually concentrated spatially in the upper levels of the trees and spectrally in the first band. This sorting result allows the 3-D SPIHT algorithm to encode the coefficients efficiently.

3. Experimental Results

In the experiments, Area-P Landsat TM images, including seven-band multispectral data with a size of 512×400 pixels with eight bits per pixel, were used. Bands 1-5 and band 7 had a 30×30 spatial resolution. The thermal Band 6 had a 120×120 spatial resolution, therefore, it was not considered in the experiment. Fig 4 shows the original image of band 5 used in the current experiment. A four-level WT was performed based considering the size of the baseband for classification and the tree structure for the SPIHT algorithm. The variance and interband correlation matrix for the feature band selection were calculated. Table I shows the variance in the baseband, while table II presents the interband correlation coefficient matrix in the baseband. Band 2 was selected as the feature band, as shown in tables I and II.

Fig. 5 shows the reference values used for the classification in the baseband. The class information was then extended to the other subbands based on considering the spatial correlation and resolution, as shown in Fig. 6. The fixed prediction coefficients for the interband prediction were obtained from several training images, including various geographical regions, such as forest, sea, rivers, mountains, roads, and residential areas, etc. One band included 13 subbands in the four-level WT domain and 13 kinds of 6×6 covariance matrix were obtained, excluding band 6. Table III shows the covariance matrix of the residual images in the baseband.

A number of experiments were performed to compare the proposed algorithms with various conventional algorithms. The simulation results showed that the proposed algorithm outperformed the conventional algorithms as regards the average PSNR at an equal bit rate, as shown in table IV.

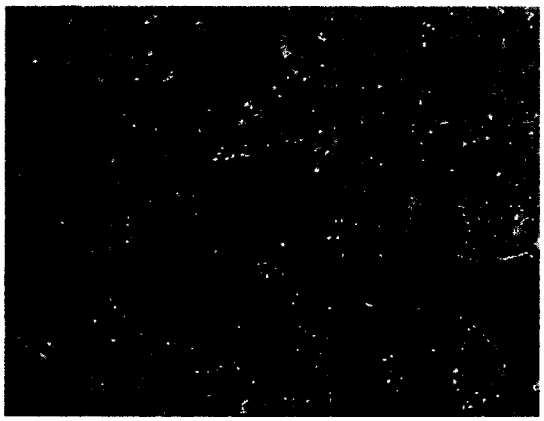

Fig. 4. Band 5 of original image.

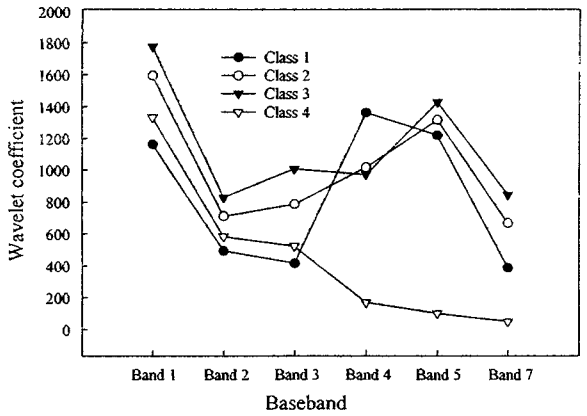

Fig. 5. Reference value of wavelet coefficients in baseband of four-level WT domain.

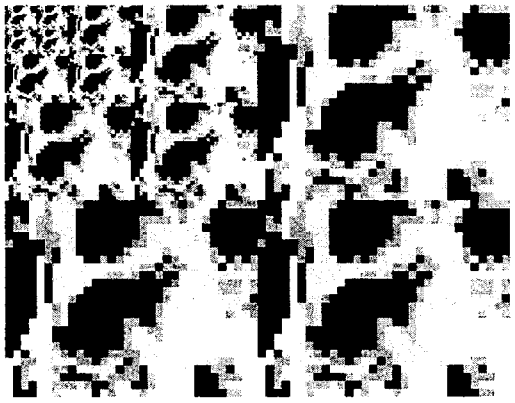

Fig. 6. Classification in baseband and its extension to subbands for Area-P.

Table I. Variance in baseband.

Band	1	2	3	4	5	7
Variance	12200	4768	14437	32172	40483	18200

Table II. Interband correlation coefficient matrix.

Band	1	2	3	4	5	7
1	1.000	0.963	0.956	0.291	0.481	0.825
2		1.000	0.991	0.164	0.524	0.804
3			1.000	0.174	0.530	0.813
4				1.000	0.632	0.191
5					1.000	0.872
7						1.000

Table III. Covariance matrix of residual image data in baseband.

Band	1	2	3	4	5	7
1	2701	139	48	-3397	-2421	174
2		83	128	75	155	129
3			1541	173	866	785
4				40829	31276	8584
5					41733	16535
7						8414

Table IV. PSNR comparison with images reconstructed using conventional methods at equal bit rate.

Bit rate [bpp]	Average PSNR [dB]			
	Proposed method	FPVQ[1]	CKLT-DCT[2]	WT-KLT[3]
0.1	32.52	29.84	30.82	31.70
0.2	35.00	32.23	32.23	34.51
0.3	36.37	33.38	33.77	36.09
0.4	37.59	34.50	34.66	37.47
0.5	38.65	34.82	34.96	38.49

4. Conclusions

The current paper proposed a new multispectral image data compression algorithm. When compared to conventional algorithms, the proposed algorithm can efficiently reduce the spectral redundancies by applying classified interband prediction in the WT domain and a KLT for the prediction errors. As a result of the WT and KLT, the transform coefficients are listed in a descending order spatially and spectrally for efficient exploitation by the 3D-SPIHT algorithm. A high prediction correctness is important in the proposed algorithm as a more accurate prediction and reduced residual image result in a better compression ratio. Accordingly, work is currently underway to effectively reduce the residual image so as to further improve the multispectral image data compression efficiency.

References

[1] S. Gupta and A. Gersho, "Feature predictive vector quantization of multispectral images," *IEEE Trans. Geosci. Remote Sensing*, vol. 30, no. 3, pp. 491-501, May 1992.

[2] G. Gelli and G. Poggi, "Compression of multispectral images by spectral classification and transform coding," *IEEE Trans. Image Processing*, vol. 8, no. 4, Apr. 1999.

[3] P. L. Dragotti, G. Poggi, and A. R. P. Ragozini, "Compression of multispectral images by three-dimensional SPIHT algorithm," *IEEE Trans. Geosci. and Remote Sensing*, vol. 38, no. 1, Jan. 2000.

[4] J. M. Shapiro, "Embedded image coding using zerotrees of wavelet coefficients," *IEEE Trans. Signal Processing*, vol. 41, no. 12, pp. 3445-3462, Dec. 1993.

[5] A. Said and W. A. Pearlman, "A new fast and efficient image codec based on set partitioning in hierarchical trees," *IEEE Trans. Circuits Syst. Video Technol.*, vol. 6, no. 3, pp. 243-250, June 1996.

[6] J. A. Saghri, A. G. Tescher, and J. T Reagon, "Practical transform coding of multispecral imagery," *IEEE Signal Processing Mag.*, pp. 32-43, Nov. 1995.

[7] G. Fernandez and C. M. Wittenbrink, "Coding of spectrally homogeneous regions in multispectral image compres-sion," in *Proc. Image Processing*, vol. 2, pp. 923-926, 1996.